FIELD INTERFERENCE OF MAGNETS IN THE LARGE ACCEPTANCE STORAGE RING CR OF THE FAIR PROJECT*

O. Gorda, C. Dimopoulou, A. Dolinskii, F. Nolden, M. Steck,
GSI, Darmstadt, Germany

Abstract

The close arrangement of the large aperture dipole and quadrupole magnets in the CR storage ring makes the overlap of the edge fields unavoidable. In addition, corrector magnets are planned to be installed in the drift sections between the dipoles and quadrupoles. 3D magnetic field simulations have been performed to quantify the effect of the field interference. This paper reports on the technique and results of the simulations. The impact of the field interference on the beam dynamics is finally discussed.

INTRODUCTION

The large acceptance storage ring CR [1] is planned to be used for cooling of antiproton and rare isotope beams at the future FAIR accelerator facility [2]. Large aperture magnets are needed in order to provide the injection of hot beams coming from separators with beam emittances up to 240 mm mrad and momentum spread up to 6%. For the CR, 36 quadrupole magnets with a horizontal aperture of 40 cm and a vertical of 18 cm are planned to be installed. Also 24 dipole magnets have a vertical gap of 17 cm together with a horizontal pole gap of 48 cm. The distance between the dipoles and quadrupoles in the CR arcs is about 60 cm that is comparable with the physical apertures of the magnets. The fringe field extends much further in magnets with larger aperture. Therefore the interference among the magnets is unavoidable if the iron-to-iron distance is 60 cm. For the CR, the dipole and quadrupole magnets are designed [3] to have a field quality better than $2 \cdot 10^{-4}$ and $5 \cdot 10^{-4}$ respectively. The field interference can change the field quality of these magnets considerably.

In addition, small dipole correctors are planned to be installed between the dipoles and quadrupoles in the arcs of the CR. The presence of the corrector iron can play a significant role since it leads to a change in the magnetic field distribution in the space between the dipole and quadrupole magnets. As a result of such an interference the field quality can be perturbed.

3D simulations of the magnetic field for the dipole and quadrupole magnets separately and two magnets combined together have been performed. The derived field maps are used to calculate the corresponding sets of multipole components. These multipole components are then applied to the beam dynamics calculations in order to quantify the effect of the field interference. As an example, the impact of the magnetic field interference on the beam dynamics in antiproton (pbar) operation mode is considered.

STUDIES OF FIELD INTERFERENCE

3D Model of the Dipole and Quadrupole Magnets

To study the distortions of the magnetic field due to a close arrangement of the dipole and quadrupole magnets the field maps are calculated in the following steps:

1) 3D field map of the dipole magnet alone is calculated.
2) 3D simulation is done for the single quadrupole magnet without any neighbouring iron.
3) Both the dipole and quadrupole magnets are combined in one 3D model as shown in Fig. 1 and the corresponding field map is calculated.
4) The iron of the dipole corrector is added in the drift space between the dipole and quadrupole magnet.

Analyzing the integrated field dependencies calculated for each of the magnets separately with those derived for the magnets combined together one can obtain changes in both the field distribution and its multipole components.
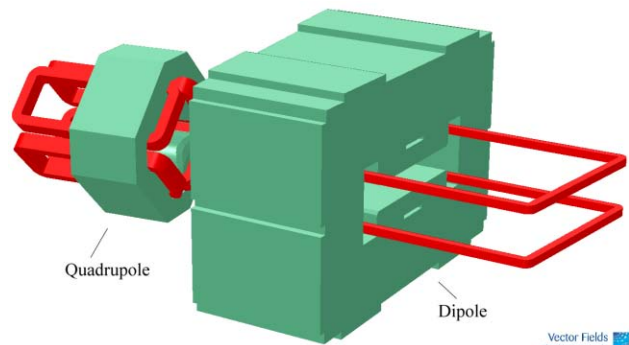

Figure 1: Simulation model of the dipole and quadrupole.

The geometry of the CR magnets and their arrangement with respect to each other corresponds to the actual lattice design [1, 4]. For symmetry reasons, each of the magnets is represented by half the length of the yoke. The OPERA-3D computer code [5] is used both to simulate the field map for each step and to evaluate field errors.

In Fig. 2 the vertical field as a function of axial position z at a radius of 20 cm calculated for each magnet separately (steps 1 and 2) is shown. One can see that the edge field fall-offs are extended to distance of about a two times the vertical aperture of the corresponding magnet. Since these magnets are placed at the distance of 60 cm to each other an overlapping of the fringe fields occurs (Fig. 2).
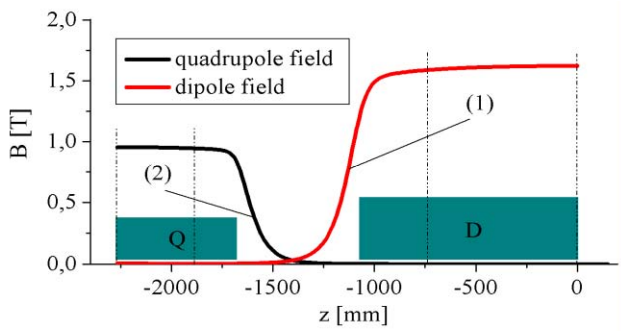
Figure 2: Magnetic field distribution in the dipole and quadrupole magnets at R_{ref} = 20 cm.

To extract multipole components and to see the difference between the different cases the calculated field maps are analyzed at a radius of 7 cm. In Table 1 three sets of the multipole components are given.

Table 1: Field integral harmonics at a reference radius of R_{ref} =7 cm, in units $10^{-4}\,m^{-(n-1)}$. n = 1, 2, 3.. corresponds to the dipole, quadrupole, sextupole comp. etc. All values are normalized with respect to the dipole component 1.6 T.

n	Quadrupole (step 1)	Dipole (step 2)	Dipole+ Quadrupole (step 3)
1	-0.5065	1.0E+4	1.0E+4
2	0.1E+4	4.3672	0.1E+4
3	1.6502	0.4692	2.6805
4	0.7172	0.1151	0.8853
5	0.3764	-0.3078	0.2642
6	0.2451	0.0157	0.2657
7	0.1562	0.1027	0.2492
8	0.1128	-0.0194	0.1458
9	0.0933	-0.0206	0.0244
10	0.0677	0.0155	0.0484

It should be noted that the set of multipoles for step 3 is not represented as a superposition of the two sets corresponding to steps 1 and 2. This indicates a noticeable change in the set of harmonics if two magnets are considered together. As an example the sextupole component becomes larger than the simple sum of the corresponding values which are obtained for the quadrupole and dipole magnet separately.

Impact of the Corrector Magnet

The simulation model of the dipole and quadrupole magnets (step 3) is modified by adding the yoke of the corrector magnet as shown in Fig.3 (step 4). Within the model, the corrector magnet has an effective iron length of 30 cm and no magnetic field inside. Only the iron core is considered to simulate its influence on the magnetic field distribution and field harmonics. The iron-to-iron distance between the dipole and quadrupole magnet is fixed at 60 cm.
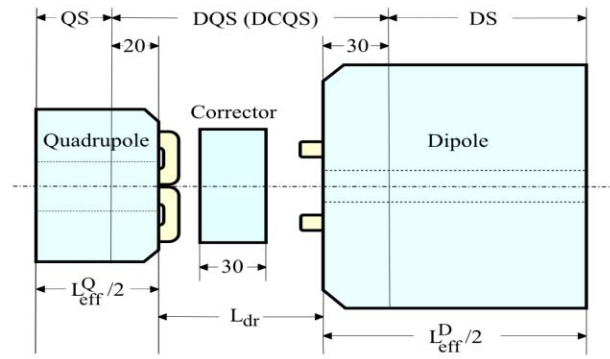

Figure 3: Schematic view of the dipole, corrector and quadrupole model.

The vertical field of the magnets as a function of the axial position z is shown in Fig.4. The black curve (3) represents the distribution without iron core and the red one (4) corresponds to the simulation model with the dipole corrector.
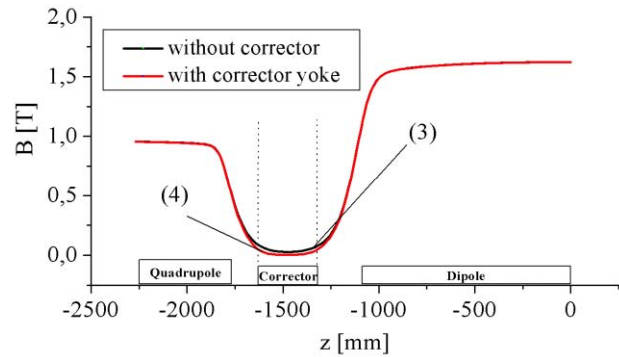

Figure 4: Magnetic field distribution at R_{ref} = 20 cm.

The presence of additional iron between the magnets results in a change of the flux path direction in the place where the iron is located. One can see that in our case the iron core decreases slightly the magnetic field inside the corrector aperture (by about 9 %).

To evaluate field harmonics the field map is analyzed separately in three regions shown in Fig. 3: QS - quadrupole section, DS - dipole section, DQS (DCQS) - section between the dipole and quadrupole magnet without (with) the iron core of the corrector magnet. The length of the QS and DS sections is smaller then the corresponding iron length of the magnets as shown in Fig. 3. Table 2 represents the sets of multipole components obtained for DQS and DCQS. The field harmonics derived for the QS and DS do not differ from the ones given in Table 1, which are obtained for the corresponding magnets.

BEAM DYNAMICS OF THE CR

Betatron Tunes

The multipole components listed in Tables 1 and 2 are used in ion-optical calculations of the CR. Obviously a

redistribution of the magnetic field due to interference effect leads to changes in the optical properties of the storage ring.

Table 2: Integral field harmonics "section-by-section", in units 10^{-4}T m$^{-(n-1)}$.

n	QDS	DCQS
1	-	-
2	-	-
3	-0.7942	-0.7674
4	-0.8751	-0.4332
5	-0.6863	-0.6751
6	-0.2947	-0.2742
7	-0.0963	-0.1084
8	-0.2587	-0.2626
9	-0.0206	-0.0194
10	0.2753	0.2915

Fig. 5 illustrates how the betatron tunes are shifted in the resonance diagram if field errors of the magnets are included. The blue curve represents the tune spread for particles with a momentum spread of 6% in linear optics, when only a chromaticity correction is applied. The red curve is the tune spread including the field errors of the magnets. The field interference changes the tune spread slightly as represented by the black curve in Fig. 5.
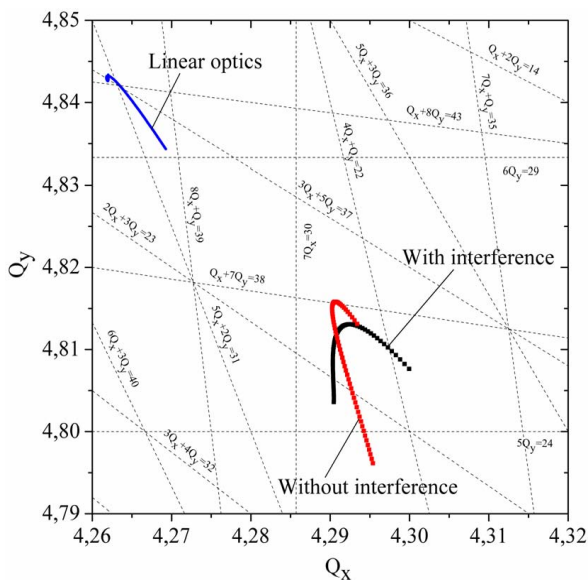

Figure 5: Tune variation for $\Delta p/p = \pm 3\%$.

Dynamic Aperture

To check the influence of the interference effect on the dynamic aperture in the CR a series of calculations have been performed using the Polymorphic Tracking Code (PTC) [6] integrated into MAD-X [7]. Some results of the simulations are plotted in Fig. 6. A significant reduction of the dynamic aperture for off-momentum particles is found. The black curves in Fig. 6 correspond to calculations including the field harmonics given in

Table. 2. One can see that taking the field inteference of magnets into account does not result in the decrease of the dynamic aperture. We even observe a small dynamic aperture growth. This can be explained by the fact that the multipole components due to the field interference lead to a small compensation of the field errors in the magnets.
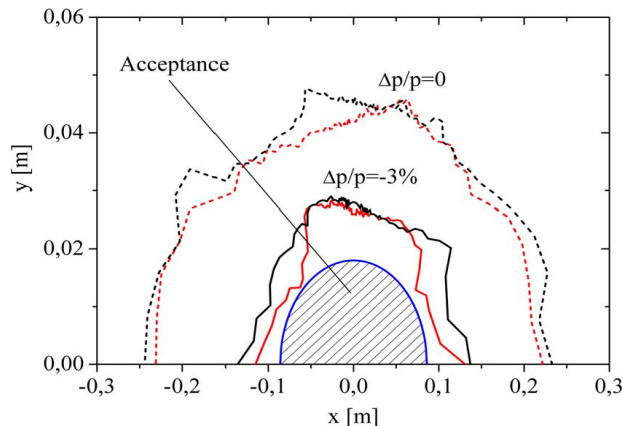

Figure 6: Dynamic aperture of the CR for 5000 turns.

SUMMARY

3D computations have been performed to quantify the effect of the field interference of the dipole and quadrupole magnets in the CR storage ring. This effect results in a change of the integral field harmonics of the simulation model. Its impact on the beam dynamics has been evaluated. Horizontal and vertical tune shifts can appear due to the field interference. The results do not show any harmful effect on the beam dynamics of the CR. In this particular case, field interference leads to a slight compensation of the field errors of the magnets resulting in a small increase of the dynamic aperture of the ring.

REFERENCES

[1] A. Dolinskii, O. Gorda, D. Obradors-Campos, S. Litvinov, F. Nolden, C. Peschke, M. Steck, I. Schurig, "The CR-RESR storage ring complex of the FAIR project", this conference, THPC011.

[2] An International Accelerator Facility for Beams of Ions and Antiprotons, Conceptual Design Report, GSI, 2006. Available at www.gsi.de/fair/reports.

[3] A. Kalimov, "Design of the CR dipole and quadrupole magnets", GSI internal notes, 2004-2005.

[4] A. Dolinskii, F. Nolden, M. Steck, "Lattice considerations for the collector and the accumulator ring of the FAIR project", COOL07, Bad-Kreuznach, September, 2007, TUA2C08, p. 106 (2007).

[5] www.vectorfields.com.

[6] F. Schmidt, "MAD-X PTC integration", PAC 2005, MPPE012, p. 1272 (2005).

[7] http://mad.web.cern.ch/mad